PHYSICAL REVIEW B VOLUME 44, NUMBER 12 15 SEPTEMBER 1991-II

Low-frequency Raman scattering from small silver particles embedded in SiO_2 thin films

M. Fujii
Division of Science of Materials, The Graduate School of Science and Technology, Kobe University, Rokkodai, Nada, Kobe 657, Japan

T. Nagareda, S. Hayashi, and K. Yamamoto
Department of Electronic Engineering, Faculty of Engineering, Kobe University, Rokkodai, Nada, Kobe 657, Japan
(Received 31 May 1991)

Intense, low-frequency Raman scattering from localized acoustic vibrations of small, spherical Ag particles embedded in SiO_2 thin films has been observed. It was found that the Raman peak shifts to higher frequencies as the particle size decreases. For Ag particles smaller than 4 nm, the size dependence of the peak frequency can be well explained by Lamb's theory, which gives vibrational frequencies of a homogeneous elastic body with a spherical form. The Raman scattering observed is relatively strong and believed to be enhanced by the excitation of the surface plasmons localized in the Ag particles; the enhancement mechanism is analogous to the case of surface-enhanced Raman scattering from molecules adsorbed on rough metal surfaces.

I. INTRODUCTION

Microcrystals as small as a few nanometers, usually called quantum dots, are currently attracting much interest, because they show optical properties much different from bulk crystals. Their distinct optical properties stem from the three-dimensional confinement of electrons and holes in small volumes (quantum size effect) (Refs. 1–5) as well as that of phonons.[6–11] The interaction between the confined electrons and phonons is also an important factor that determines the optical properties.[4,5] Until now, the effects of confinement on optical phonons have been studied by Raman spectroscopy. For GaP microcrystals, Hayashi and Kanamori[6] have demonstrated that a surface-phonon mode appears between TO- and LO-phonon modes. For optical phonons in nonpolar microcrystals such as Si and Ge microcrystals, size-dependent shifts and broadening have commonly been observed.[7–11]

In this paper, we are concerned with Raman scattering from confined acoustic phonons rather than the confined optical phonons. The Raman study of confined acoustic phonons has been initiated only recently. Duval, Boukenter, and Champagnon[12] have reported the appearance of a low-frequency Raman peak around 10 cm^{-1} for nucleated glasses containing microcrystals as small as 10 nm. From a comparison with theoretical eigenfrequencies derived from the theory of Lamb,[13] which describes elastic vibrational modes of a sphere, they attributed the observed low-frequency Raman peak to an acoustic-phonon mode confined in the microcrystals. Similar low-frequency Raman peaks have been observed so far for microcrystalline (μc) Ge embedded in GeO_2 matrices,[14] μc-Ag in alkali halide,[15] and μc-CdS_xSe_{1-x} in SiO_2.[16]

In spite of these Raman studies, characterization of the samples was not sufficient. The microcrystalline samples studied so far had some deficiencies to directly compare the experimental result with Lamb's theory. First, the size of the microcrystals could not be systematically controlled. Second, the shape of the microcrystals was not spherical and the shape distribution was relatively wide. Third, in the case of nucleated glasses, the composition and structure of the microcrystals were very complicated and accurate sound velocities in the microcrystals were not available.

The purpose of this work is to study low-frequency Raman scattering for much simpler systems and clarify the relationship between microcrystalline size and Raman peak frequency. We have succeeded in preparing small silver particles embedded in SiO_2 thin films and clearly observing the low-frequency Raman scattering. The size of Ag microcrystals could be systematically controlled from 2.5 to 5 nm in diameter by changing the volume ratio of Ag to SiO_2 in the samples. Transmission electron microscopic (TEM) observations revealed that the Ag microcrystals are almost spherical and well dispersed in the matrices. We compare the observed peak frequencies with the results of theoretical calculations based on Lamb's theory. It is shown that the peak frequencies agree fairly well with the theoretical results if the particle size is less than about 4 nm. We also discuss the enhancement of the Raman intensity by a strong electric field induced by the surface-plasmon resonance of Ag microcrystals.

II. EXPERIMENT

Samples were prepared by a rf cosputtering method similar to that used in our previous work on Ge microcrystals embedded in SiO_2 thin films.[10,11] Small pieces of Ag tips ($0.5\times2.5\times5$ mm^3) were placed on a sputtering target of pure SiO_2 (10 cm in diameter) and they were cosputtered in Ar gas of 2.7 Pa with a rf power of 200 W. An ANELVA SPF210H sputtering apparatus was used. The substrates used were Si wafers for Raman measurements, cleaved KBr plates for electron microscopy, and

fused-quartz plates for optical transmission measurements. During the deposition the substrates were not intentionally heated. After the deposition, the films on the KBr plates were wet-stripped and mounted on electron microscopic grids. In this preparation method, the size of Ag microcrystals is controllable by changing the volume ratio of Ag to SiO_2. The volume ratio was varied by changing the number of Ag targets on the SiO_2 target at the moment of sputtering. The film thickness was so adjusted that the total volume of Ag in all the samples remains roughly the same. The film thickness was in the range between 0.4 and 2.7 μm for Raman measurements and 0.1 and 0.3 μm for optical transmissions measurements. The thickness of the samples for electron microscopy was fixed at 30 nm.

Raman measurements were carried out in a conventional 90° scattering geometry at room temperature. The spectra were excited by the 514.5- and 488.0-nm lines of an Ar-ion laser and recorded by a Spex Ramalog 5M spectrophotometer equipped with a double monochromator and photon-counting system. To investigate polarization properties, we observed polarized ($I_{\parallel}$) and depolarized ($I_{\perp}$) spectra at $X(ZZ)Y$ and $X(ZX)Y$ geometries, respectively, where the X axis is taken for the direction of the laser beam with its electric vector in the Z direction and the Y axis for the direction of scattered light. Electron microscopic images were obtained by operating a JEM-200CX electron microscope at 200 kV. Throughout this work, the average sizes were determined directly from TEM images. Optical transmission spectra were measured by a conventional setup including a tungsten lamp, Nikon 250G monochromator, photomultiplier, and NF LI-570 lock-in amplifier.

III. RESULTS AND DISCUSSION

A. Electron microscopy

Figures 1(a)–1(c) show TEM images of Ag microcrystals embedded in SiO_2 thin films. Dark patches in these figures correspond to Ag microcrystals. The volume fraction of Ag in the sample shown in Fig. 1(a) is about 1.5 times larger than that shown in 1(b), and about 3 times larger than that shown in 1(c). These figures clearly demonstrate that as the volume fraction of Ag decreases, the average particle size decreases; the average diameters are 5.2, 4.1 and 2.8 nm for Figs. 1(a)–1(c), respectively. As can be seen in these figures, the microcrystals are almost spherical and well dispersed in the matrices.

Figures 2(a)–2(c) show the size distributions of Ag microcrystals obtained from Figs. 1(a)–1(c), respectively.

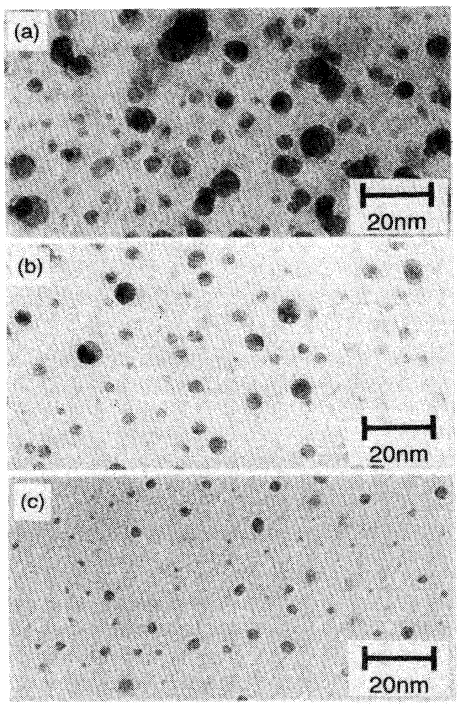

FIG. 1. Electron microscopic images of Ag microcrystals embedded in SiO_2 thin films. Average particle diameters are (a) 5.2 nm, (b) 4.1 nm, and (c) 2.8 nm.

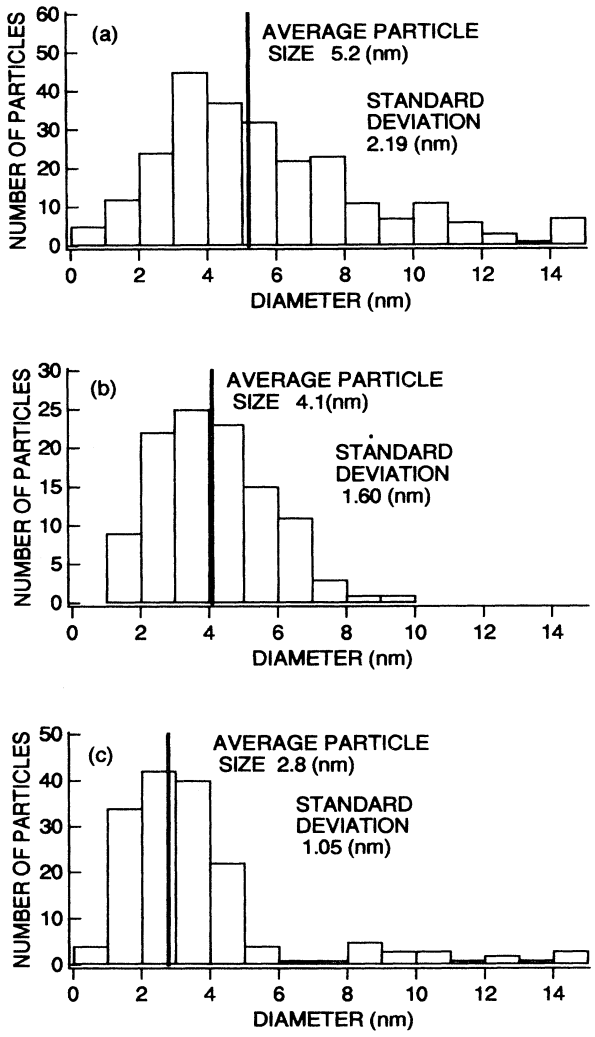

FIG. 2. Size distribution of Ag microcrystals embedded in SiO_2 thin films. (a)–(c) are obtained from TEM images shown in Figs. 1(a)–1(c).

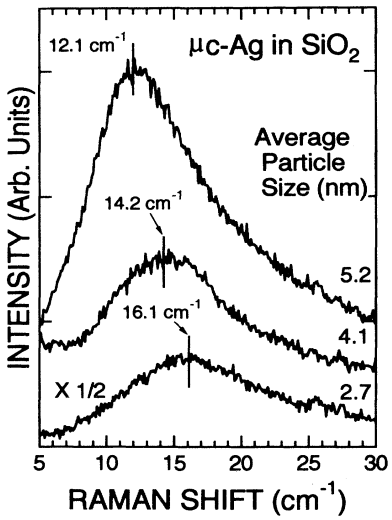

FIG. 3. Raman scattering from Ag microcrystals embedded in SiO_2 thin films.

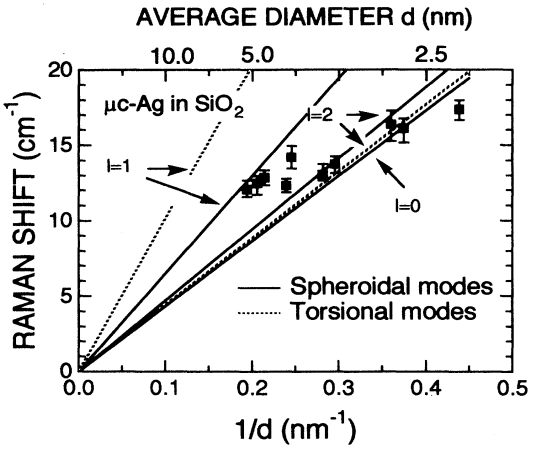

FIG. 5. Peak frequency of very low-frequency Raman scattering as a function of an inverse particle diameter. Solid and dashed lines are the results of theoretical calculations for spheroidal and torsional modes, respectively.

The samples with the average sizes of 2.8 and 4.1 nm [Figs. 2(c) and 2(b)] show relatively narrow size distributions with standard deviations of 1.05 and 1.60 nm, respectively. In contrast to this, the size distribution in Fig. 2(a) is very broad and has a tail toward the larger size. The standard deviation of the sample in Fig. 2(a) is 2.19 nm. In the present work the size distribution was found to be always broader for larger average size (i.e., for larger volume fraction of Ag in the films).

B. Size dependence of Raman scattering

Figure 3 shows the size dependence of the low-frequency Raman spectrum for the small silver particles measured with the 514.5-nm excitation. The sample with $d=5.2$ nm exhibits a relatively sharp peak at 12.1 cm^{-1}, which is asymmetric, having a long tail toward the high-frequency side. The peak is rather strong and is several times as intense as the optical-phonon peak for polished Si(100) surfaces at 520 cm^{-1} measured under the same experimental condition. As the size decreases, the peak shifts to higher frequencies and reaches 16.1 cm^{-1} for $d=2.7$ nm. Furthermore, the width of the peak increases gradually and the peak becomes symmetric. The intensity of the peak also decreases rapidly with decreasing size, although the total volume of Ag in all the samples is fixed roughly the same. The spectra obtained with the 488.0-nm excitation were almost identical with those shown in Fig. 3; no excitation energy dependence of the peak frequency was observed in the present work.

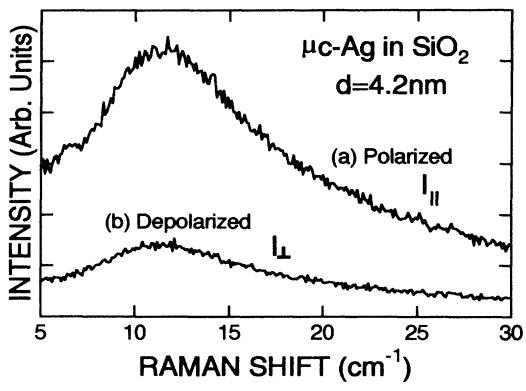

FIG. 4. (a) Polarized ($I_{\parallel}$) and (b) depolarized ($I_{\perp}$) Raman spectra for Ag microcrystals with $d=4.2$ nm.

Figure 4 shows polarized [4(a)] and depolarized [4(b)] Raman spectra for the sample with $d=4.2$ nm. Both spectra exhibit a peak with almost the same shape. We have performed the same studies for some other samples, but observed no change in the spectral shape for polarized and depolarized spectra. The depolarization factor of the peak in Fig. 4 is about 0.27. The depolarization factor was found to be almost independent of the particle size.

Figure 5 plots the Raman peak frequency as a function of the inverse diameter. Solid and dashed lines represent calculated results explained later. In the figure, we can see that the peak frequency strongly depends on the particle size and monotonously increases with decreasing size.

C. Calculation of vibrational eigenfrequencies for a homogeneous elastic sphere

The low-frequency Raman scattering from a microcrystal is considered to be due to an elastic vibration of the microcrystal itself. Lamb,[13] Nishiguchi and Sakuma,[17] and Tamura, Higeta, and Ichinokawa[18] have theoretically studied the vibrational eigenfrequencies of a homogeneous elastic sphere with a free surface (i.e., eigenfrequencies of confined acoustic modes). Two eigenequations were derived as

$$j_{l+1}(\eta)-\frac{l-1}{\eta}j_l(\eta)=0 \quad (l\geq 1) \quad \text{(torsional mode)}\,, \tag{1}$$

$$2\left[\eta^2+(l-1)(l+2)\left[\frac{\eta j_{l+1}(\eta)}{j_l(\eta)}-(l+1)\right]\right]\frac{\xi j_{l+1}(\xi)}{j_l(\xi)}-\frac{\eta^4}{2}+(l-1)(2l+1)\eta^2$$
$$+[\eta^2-2l(l-1)(l+2)]\frac{\eta j_{l+1}(\eta)}{j_l(\eta)}=0 \quad (l\geq 0) \quad \text{(spheroidal mode)}\,, \tag{2}$$

where η and ξ are nondimensionalized eigenfrequencies and l is an angular momentum quantum number. The solutions of Eq. (1) give eigenfrequencies of the torsional oscillations without dilatation and those of Eq. (2) give those of the spheroidal motions with dilation. The torsional modes are characterized by the quantum number $l=1,2,3,\ldots$, and corresponding eigenfrequencies η_l^t are written as

$$\eta_l^t=\frac{\omega_l^t d}{2v_t}\,, \tag{3}$$

where ω_l^t is the angular frequency of the lth torsional mode, v_t is the transverse sound velocity, and d is the diameter of the microcrystal. The spheroidal modes are characterized by $l=0,1,2,\ldots$, and corresponding eigenfrequencies (η_l^s and ξ_l^s) are written as

$$\eta_l^s=\frac{\omega_l^s d}{2v_t}\,, \quad \xi_l^s=\frac{\omega_l^s d}{2v_l}\,, \tag{4}$$

where v_l is the longitudinal sound velocity. Here, we should note that the nondimensionalized eigenfrequencies of the spheroidal modes (η_l^s and ξ_l^s) strongly depend on the material through the ratio v_t/v_l, while those of the torsional modes (η_l^t) do not depend on the material.

Using Eqs. (1) and (2), we have calculated the values of η_{ln}^t and η_{ln}^s, which are the $(n+1)$th eigenvalues belonging to the angular momentum l. Only the lowest modes ($n=0$) are the surface modes and higher modes ($n\geq 1$) are the inner modes.[18] The sound velocities of Ag used are $v_l=3650$ m/s and $v_t=1660$ m/s.[19] The Raman peak frequencies of the torsional and spheroidal modes with $n=0$ can be expressed as

$$\omega_t^1=1.83\frac{v_t}{dc}\,, \quad \omega_t^2=0.80\frac{v_t}{dc}\,, \tag{5}$$

$$\omega_s^0=0.36\frac{v_l}{dc}\,, \quad \omega_s^1=1.17\frac{v_t}{dc}\,, \quad \omega_s^2=0.84\frac{v_t}{dc}\,, \tag{6}$$

where ω_t^1 and ω_t^2 are the Raman peak frequencies of the torsional modes with $l=1$ and 2, respectively, ω_s^0, ω_s^1, and ω_s^2 are those of the spheroidal modes with $l=0$, 1, and 2, respectively, and c is the vacuum light velocity. Equations (5) and (6) demonstrate that the Raman shifts of both modes are proportional to the sound velocities and inversely proportional to the diameter of the particle.

Among various vibrational modes, only the modes with even parity can be Raman active. Duval, Boukenter, and Champagnon claimed that all the modes with even l are Raman active.[12,15,16] However, as described in the following, our analysis does not predict such a selection rule. The displacement vectors of the two types of vibrational modes ($\mathbf{u}_t$ and $\mathbf{u}_s$ for torsional and spheroidal modes, respectively) can be expressed by one scalar (ϕ_0) and two vector potentials ($\boldsymbol{\phi}_1$ and $\boldsymbol{\phi}_2$) as

$$\mathbf{u}_t=\nabla\times\boldsymbol{\phi}_1\,, \tag{7}$$

$$\mathbf{u}_s=\nabla\phi_0+\nabla\times\nabla\times\boldsymbol{\phi}_2\,, \tag{8}$$

where $\boldsymbol{\phi}_i=(r\phi_i,0,0)$; ϕ_0, ϕ_1, and ϕ_2 are scalar functions.[13,17,18] From Eqs. (7) and (8) it follows that the parity of the $\mathbf{u}_t$ is opposite to that of ϕ_1, and that of the $\mathbf{u}_s$ is the same as those of ϕ_0 and ϕ_2. The scalar functions ϕ_0, ϕ_1, and ϕ_2 are proportional to the spherical harmonics $Y_l^m(\theta,\phi)$. The spherical harmonics with even l are even, and those with odd l are odd. Therefore the spheroidal modes with $l=0,2,4,\ldots$ and the torsional modes with $l=1,3,5,\ldots$ can be Raman active at first order. In the case of the spheroidal mode with $l=0$, Raman scattering is expected to be completely polarized and in other cases partially depolarized.

D. Comparison between theory and experiment

Solid and dashed lines in Fig. 5 represent the calculated Raman peak frequencies for the lowest-energy ($n=0$) spheroidal and torsional modes respectively [Eqs. (5) and (6)]. The spheroidal modes with $l=0,2$, which are Raman active, have almost the same slope. The modes with $l=1$ show larger slope. Our calculations show that the surface modes ($n=0$) with $l\geq 3$ and all inner modes ($n\geq 1$) exhibit larger slope than that of the spheroidal mode with $l=1$. In Fig. 5, a fairly good agreement between experiments and calculations for spheroidal modes with $l=0$ and 2 can be seen for the microcrystals smaller than 4 nm. This agreement allows us to conclude that the observed low-frequency Raman scattering is due to the confined acoustic phonons in Ag particles, which are quantized by the confinement effects.

It should be possible to specify the observed mode as $l=0$ or 2 from the polarization properties, because the spheroidal mode with $l=0$ is expected to be completely polarized and all other modes are partially depolarized. The depolarization factor presently observed was not zero (about 0.27) for all the samples. This seems to suggest that the observed peak is due to the $l=2$ mode. However, the $l=0$ mode is completely polarized only if the particle is perfectly spherical. As can be seen in Fig. 1, our samples are almost spherical but not perfectly spherical. This may result in a nonzero depolarization factor for the $l=0$ mode. Therefore we cannot unambiguously identify the observed mode from the depolariza-

tion factor. In order to quantitatively discuss the depolarization factor of the confined acoustic modes, further theoretical studies are required

As shown in Fig. 4, we have observed almost the same spectral shape for polarized ($I_{\parallel}$) and depolarized ($I_{\perp}$) spectra. This disagrees with the Raman results for ellipsoidal Ag particles studied by Mariotto *et al.*[15] They observed much different spectra for $I_{\parallel}$ and $I_{\perp}$; two peaks appear on the $I_{\parallel}$, while only one peak appears on the $I_{\perp}$. From this polarization property, they assigned the Raman peaks to the spheroidal mode with $l=2$. In general, the lth mode is $(2l+1)$ degenerate. The $l=2$ mode is thus fivefold degenerate and, in the case of ellipsoidal shape, m degeneracy is partially lifted and three quadrupolar modes corresponding to $m=0$, ± 1, and ± 2 are observed. Since the depolarization factor of these modes is different from each other, they observed different spectral shape for $I_{\parallel}$ and $I_{\perp}$. In the present samples, Ag microcrystals are almost spherical and thus the vibrational modes are almost degenerate, resulting in the same spectral shape for $I_{\parallel}$ and $I_{\perp}$ regardless of the vibrational modes.

In the case of microcrystals larger than about 4.0 nm, the agreement between experiments and calculations becomes rather poor. The experimental Raman shifts are always larger than those of theoretical predictions. Although the reasons for the discrepancy are not clear at present, a possible reason is a wide size distribution. As shown in Fig. 2, the size distribution is very narrow for the microcrystals with small average size, but this becomes very broad as the average size increases (typically for $d>4.0$ nm). Furthermore, the average size deviates about 1 nm from the top of the distribution as shown in Fig. 2(a). For the microcrystalline samples with such a broad size distribution, the average size is less meaningful and the size distribution should be taken into account in the calculations. Unfortunately, we could not make the calculations, because a theory which gives Raman intensities of confined acoustic phonons is not available at present. Another possible reason for the discrepancy between experiments and calculations is the effects of particle shape. As can be seen in Fig. 1, the shape is almost spherical for relatively small particles. However, the shape becomes rather irregular as the size increases. The deviation of microcrystalline shape from the perfect spherical form may cause the changes in the vibrational frequencies and Raman selection rules.

The theory we used for the calculations assumes that the surfaces of the microcrystals are free. However, the present Ag microcrystals are embedded in SiO_2 matrices and the surfaces are considered to be fixed by the matrices. Tamura, Higeta, and Ichinokawa[18] extended Lamb's theory and considered the various effects on the microcrystalline surfaces. They showed that the surface modes (the modes with $n=0$) disappear if Lamé's constants λ and μ and the mass density ρ of the microcrystals have close values as those of matrices. In the present work, the values of λ and ρ for Ag are much different from those for SiO_2. As shown in Fig. 5, our experimental results show a good agreement with the results of calculations obtained by assuming the free surface boundary conditions. This implies that the surface vibrational modes exist not only in freestanding microcrystals but also in buried microcrystals if λ and ρ of microcrystals are much different from those of matrices. The matrix effects may be clarified by burying Ag microcrystals in other matrices such as Al_2O_3, GeO_2, etc. Such studies are now under way in our laboratory.

In the above discussion, we assumed that the microcrystal is a homogeneous elastic body. The assumption is valid provided that the microcrystal is large enough and does not have large anisotropy in the elastic constants. The small size limit of the applicability of the continuum assumption has not yet been examined theoretically. Therefore, the validity can be judged only by comparing the theoretical results with experimental ones. The excellent agreement between experiments and calculations obtained for the present samples may indicate that the assumption is valid for the microcrystals as small as 3 nm. However, for microcrystals much smaller than the present Ag microcrystals, the continuum assumption may not be applicable and a more rigorous calculation, such as lattice-dynamical calculations, will be necessary. It seems to be very interesting to study the low-frequency Raman scattering for much smaller microcrystals and compare the results with those obtained by the lattice-dynamical calculations.

E. Enhancement of low-frequency Raman scattering by surface plasmon

As mentioned in the above, the intensity of the low-frequency peak observed is considerably strong; the peak is several times as intense as the optical-phonon peak for polished Si(100) surfaces at 520 cm^{-1}. Furthermore, the intensity depends on the particle size. The extremely intense low-frequency Raman peak was also observed for Ag electrodes with rough surfaces by Weitz *et al.*[20] They assigned the low-frequency Raman scattering to acoustic phonons localized in the rough surfaces. The Raman scattering they observed is considered to be enhanced by the surface plasmons localized in the surface roughness features; the enhancement mechanism is analogous to the case of surface-enhanced Raman scattering (SERS) of adsorbed molecules on rough metal surfaces. The protrusions in the rough surfaces have a wide shape distribution and the resonant frequency of the surface plasmon strongly depends on the shape. Therefore, under an excitation with a given wavelength, a localized acoustic mode from protrusions with a particular shape is resonantly excited. This results in a strong excitation wavelength dependence of Raman peak frequency. Weitz *et al.*[20] observed the strong excitation dependence of the peak frequency and concluded that Raman scattering from the confined acoustic phonons is enhanced by the surface plasmon.

The low-frequency Raman scattering presently observed is also considered to be enhanced by the surface plasmons localized in the microcrystals. However, no excitation wavelength dependence of peak frequency was observed in the present work because of the spherical form of our Ag microcrystals. In Fig. 6, optical absorp-

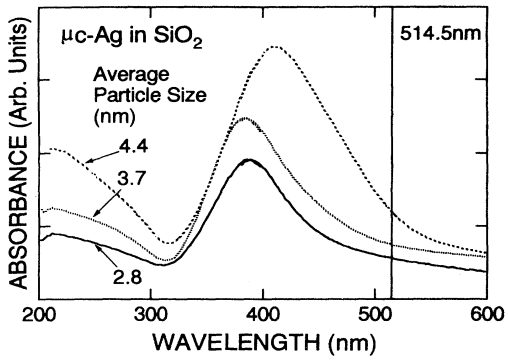

FIG. 6. Optical absorption spectra of Ag microcrystals embedded in SiO_2 thin films.

tion spectra of the Ag small particles are displayed. The peak around 400 nm corresponds to the surface-plasmon resonance. The peak is very broad, because the particle sizes are much smaller than the mean free path of electrons in the bulk metal (about 200 nm) and, in this case, electrons are scattered at particle surfaces.[21] As the microcrystalline size increases (as the volume fraction increases), the peak shifts to longer wavelength due to the increase in the electromagnetic interactions between microcrystals. Furthermore, the peak becomes stronger, although the total volume of Ag in all the samples was kept almost constant by varying the film thickness. Since we excite the Raman spectra using the 514.5-nm line, the enhancement of Raman scattering is caused by the tail region of the surface-plasmon resonance. As the size increases, the absorption at 514.5 nm increases. We believe that this is one of the causes for the observed size dependence of Raman peak intensity. We can expect much stronger low-frequency Raman scattering for an excitation around 400 nm. Such experiments would be of great interest.

IV. CONCLUSION

The localized acoustic phonons in the Ag microcrystals embedded in SiO_2 matrices were clearly observed by Raman spectroscopy. Results of TEM observations revealed that Ag microcrystals with almost spherical form are randomly dispersed in the matrices. The spherical form of our microcrystals allowed us to directly compare the observed results with Lamb's theory. We have demonstrated that the high-frequency shifts of the Raman peak with decreasing the size can be well explained by Lamb's theory. This implies that the continuum approximation is valid for Ag microcrystals as small as 3 nm. We could assign the observed Raman peak to the spheroidal mode with $l=0$ or 2.

Although Lamb's theory could well explain the observed size dependence of Raman peak frequencies, the theory is still too simple to fully account for the observed low-frequency Raman scattering. At present, no theory which deals with the Raman spectral shape, intensities, and depolarization factors of the confined acoustic phonons is available. Further theoretical and experimental studies are still required to fully understand Raman scattering from the confined acoustic phonons. Similar researches for microcrystalline Si, Ge, CdS, CdSe, CuCl, etc. embedded in SiO_2 and other matrices are currently under way and results will be published elsewhere.

ACKNOWLEDGMENTS

This work was supported by a Grant-in-Aid for Scientific Research, from the Ministry of Education, Culture and Science, Japan. We are indebted to Dr. Y. Nozue of Tohoku University for valuable discussions and suggestions.

[1]A. I. Ekimov, Al. L. Efros, and A. A. Onoushchenko, Solid State Commun. **56**, 921 (1985).
[2]A. Nakamura, H. Yamada, and T. Tokizaki, Phys. Rev. B **40**, 8585 (1989).
[3]Y. Wang, A. Suna, and J. McHugh, J. Chem. Phys. **92**, 6927 (1990).
[4]T. Itoh and M. Furumiya, J. Lumin. **48&49**, 704 (1990).
[5]M. C. Klein, F. Hache, D. Ricard, and C. Flytzanis, Phys. Rev. B **42**, 11 123 (1990).
[6]S. Hayashi and H. Kanamori, Phys. Rev. B **26**, 7079 (1982).
[7]H. Richter, Z. P. Wang, and L. Ley, Solid State Commun. **39**, 625 (1981).
[8]Z. Iqbal and S. Veprek, J. Phys. C **15**, 377 (1982).
[9]I. H. Campbell and P. M. Fauchet, Solid State Commun. **58**, 739 (1986).
[10]M. Fujii, S. Hayashi, and K. Yamamoto, Appl. Phys. Lett. **57**, 2692 (1990).
[11]M. Fujii, S. Hayashi, and K. Yamamoto, Jpn. J. Appl. Phys. **30**, 687 (1991).
[12]E. Duval, A. Boukenter, and B. Champagnon, Phys. Rev. Lett. **56**, 2052 (1986).
[13]H. Lamb, Proc. London Math. Soc. **13**, 189 (1882).
[14]N. N. Ovsyuk, E. B. Gorokhov, V. V. Grishchenko, and A. P. Shebanin, Pis'ma Zh. Eksp. Teor. Fiz. **47**, 248 (1988) [JETP Lett. **47**, 298 (1988)].
[15]G. Mariotto, M. Montagna, G. Viliani, E. Duval, S. Lefrant, E. Rzepka, and C. Mai, Europhys. Lett. **6**, 239 (1988).
[16]B. Champagnon, B. Andrianasolo, and E. Duval, J. Chem. Phys. **94**, 5237 (1991).
[17]N. Nishiguchi and T. Sakuma, Solid State Commun. **38**, 1073 (1981).
[18]A. Tamura, K. Higeta, and T. Ichinokawa, J. Phys. C **15**, 4975 (1982).
[19]*Chronological Scientific Tables*, edited by National Astronomical Observatory (Maruzen, Tokyo, 1991).
[20]D. A. Weitz, T. J. Gramila, A. Z. Genack, and J. I. Gersten, Phys. Rev. Lett. **45**, 355 (1980).
[21]S. Hayashi, R. Koga, M. Ohtuji, K. Yamamoto, and M. Fujii, Solid State Commun. **76**, 1067 (1990).

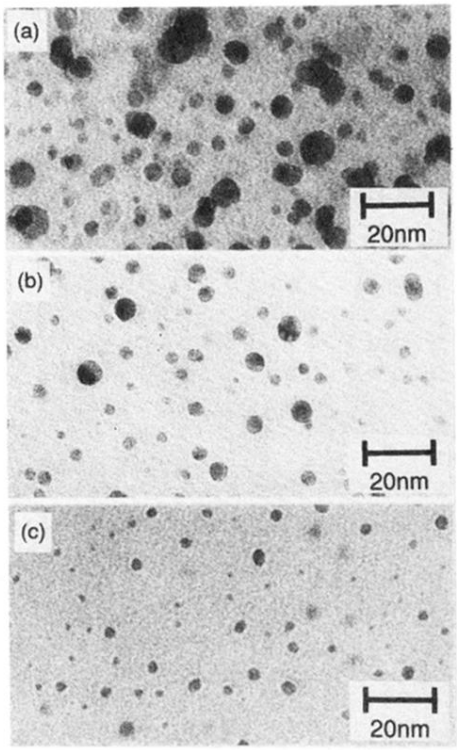

FIG. 1. Electron microscopic images of Ag microcrystals embedded in SiO_2 thin films. Average particle diameters are (a) 5.2 nm, (b) 4.1 nm, and (c) 2.8 nm.